VORTICITY GENERATED BY A DAM BREAK OVER A WET BED MODELED BY SMOOTHED PARTICLE HYDRODYNAMICS

A. J. C. Crespo[1], M. Gómez-Gesteira[1] and R.A. Dalrymple[2]
Grupo de Física de la Atmósfera y del Océano, Universidad de Vigo, Ourense, Spain;
alexbexe@uvigo.es; mggesteira@uvigo.es
[2] Department of Civil Engineering, Johns Hopkins University, Baltimore, USA; rad@jhu.edu

Abstract. Dam break evolution over dry and wet beds is analyzed in the framework of SPH (Smoothed Particle Hydrodynamics) model. The model showed to fit accurately both the experimental dam- break profiles and the measured velocities. In addition, the model allows studying different propagation regimes during the dam- break evolution. In particular, different dissipation mechanisms were identified: bottom friction and wave breaking. Although breaking dominates over wet beds at the beginning of the movement, bottom friction becomes the main dissipation mechanism in the long run. Furthermore, vorticity is studied in terms of SPH formulation for different fluid depths.

Keywords: Smoothed Particle Hydrodynamics, SPH, dam break, wet beds, and vorticity.

1. INTRODUCTION

Typical dam break experiments show a rapidly moving tongue of water generated by the instantaneous release of a given volume of water confined in a rectangular channel. The theoretical description of the two dimensional dam break problem for an inviscid fluid on a dry bed was carried out by Ritter (1892) by solving the non-linear shallow water equations. The resulting front travels downstream with a celerity $c = 2\sqrt{gd_0}$, where g is acceleration due to gravity and d_0 is the initial water depth behind the dam. Although the theoretical approach assumes no boundary friction, experiments show good agreement with the theory, except for the leading edge of the wave as bottom friction affects the leading tip significantly. Dressler (1952) added a Chezy resistance term to the momentum equation; Whitham (1955) developed an analogy between the wave front and a turbulent boundary layer. Thus, for a horizontal dry channel wave front celerity was observed to depend on time. In addition, the problem becomes much more complex when the dam break wave propagates over still water (initial depth d>0). This configuration results in a positive surge (Henderson, 1966) whose governing equations were graphically solved by Montes (1998). Thus, stationary celerity can be fitted in terms of d and d_0. In spite of theses previous studies, the dynamics of dam breaks is far from being completely understood, especially when the wave front advances over a wet bed. Apart from the theoretical interest of this configuration, it can also contribute to the understanding of tsunamigenic waves when reaching the shoreline as mentioned in Chanson *et al.* (2003).

Models based on Smoothed Particle Hydrodynamics (SPH) are an option to address dam break evolution. SPH is a purely Lagrangian method developed during seventies (Lucy, 1977; Gingold and Monaghan, 1977; Monaghan, 2005) in astrophysics to study the collision of galaxies and the impacts of bolides on planets. The numerical method has been shown to be robust and applicable to a wide variety of other fields. Recently, SPH has been used for wave impact studies on offshore structures (Fontaine, 2000; Dalrymple *et al*., 2002; Gómez-Gesteira and Dalrymple, 2004; Gómez-Gesteira *et al*., 2005).

The main advantages of SPH arise directly from its Lagrangian nature, which provides to the method some advantages compared to the usual limitations in Eulerian methods. On the one hand, the density number of particles increases in regions where the fluid is present, in

such a way that the computational effort is mainly concentrated in those regions. On the other hand, there are no constraints imposed either on the geometry of the system or in how far it may evolve from the initial conditions.

The aim of this paper is the study of the dam break experiment and the effect of wet bottom in his evolution by means of the SPH model. The method will be showed to fit accurately experimental results. In addition, the model captures most of the feature of a dam break over a wet bed, in particular it will allow analyzing the vorticity and dissipation associated to the interaction between the dam break and the still water placed near bed.

2. THE EXPERIMENT

Here we use laboratory experiments by Janosi *et al.* (2004) to validate an SPH model of dam break evolution over a wet bed. The schematic arrangement of their experimental tank, which has two parts, is shown in Fig. 1. The channel, beginning at x=38cm, is 955 cm long and 15 cm wide. The bottom and side walls of the channel were constructed with glass, the second part, comprising the lock and lock gate, is 38 cm long and made from Plexiglas. The initial fill height of the lock (d_0) for our comparisons is taken as 0.15 m. The initial water depth in the channel downstream of the lock was varied depending on the experiment.

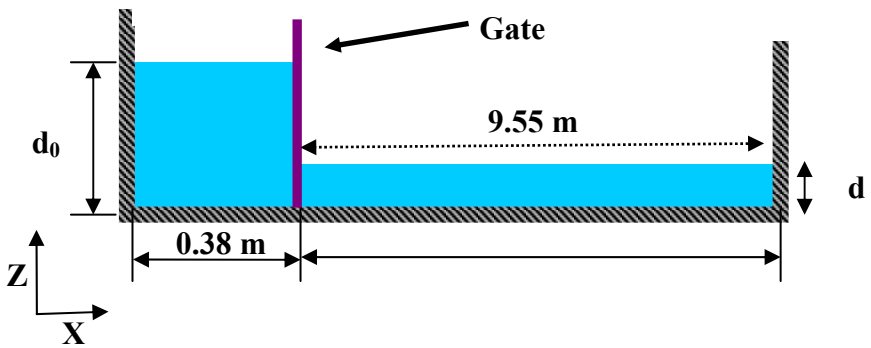

Figure 1: Schematic arrangement and geometric dimensions of the dam-break experiments.

The position of the water front as a function of time was determined from digitized pictures. The gate separating the lock from the rest of the tank was removed from above at an approximate constant velocity (V_{gate} = 1.5 ms^{-1}). The movement of this gate will be shown to play a key role when fitting numerical results to experimental ones, since the gate velocity is on the same order of magnitude as the wavefront celerity.

3. SPH METHODOLOGY

The main features of the SPH method, which is based on integral interpolants, are described in detail in Monaghan (1982), Monaghan (1992), Benz (1990) and Liu (2003) and we will only refer here to the main features of the method.

Weight functions play a fundamental role in SPH method. They should be constructed following several conditions such as positivity, compact support, normalization, monotonically decreasing and delta function behavior (Liu 2003). The cubic spline kernel developed by Monaghan and Lattanzio (1985) was used in our simulations. To avoid particle clumping, which is inherent to the chosen kernel, the tensile instability correction proposed by Monaghan (2000) was used. Using this normalized cubic spline kernel, the basic equations of conservation can be represented in SPH notation following (Monaghan 1992). In particular, the momentum equation given by Monaghan (1992) was used. Changes in the fluid density were calculated by means of the differential equation given by Monaghan (1992) instead of using a weighted summation of mass terms, which leads to an artificial density decrease near

fluid interfaces. The relationship between pressure and density was assumed to follow the equation of state given by Monaghan *et al.* (1999) according to Batchelor (1974). Particles were moved using the XSPH variant due to Monaghan (1989).

4. SPH IMPLEMENTATION

4.1. INITIAL CONDITIONS: FLUID PARTICLES

Fluid particles were initially placed on a staggered grid with zero initial velocity. Nodes of the grid are located at $\vec{R} = l\,dx\vec{i} + m\,dz\vec{k}$ with a two- point basis (0,0) and (dx/2, dz/2) referred to the corner defined by $\vec{R}$. l, and m are integers, $\vec{i}, \vec{k}$ are unitary vectors in X, Z directions and dx = dz = 0.005 m. A smoothing length, h = 0.006 m, was considered in all simulations.

The particles are assigned an initial density ρ_0 was given by

$$\rho(x,z) = \rho_0 \left(1 + \frac{\rho_0 g (H(x) - z)}{B} \right)^{1/\gamma} \tag{1}$$

where *H(x)* is the water column height at position *x* and *z* is the vertical distance from the bottom.

4.2. BOUNDARIES

Due to the particular geometry of the numerical experiment, two different boundary conditions were considered: fixed particles and gate particles. All of them are treated as *quasi* fluid particle (see Gómez-Gesteira *et al.*, 2005), since they follow the continuity equation and the equation of state, but they do not follow the momentum equation and the XSPH variant, in such a way that their position and velocity are externally fixed.

Fixed particles (including bottom and fixed walls) are placed in two rows forming a staggered grid *with dx = dz = 0.005 m* and zero initial velocity. Their positions and velocities remained unchanged during the numerical experiment.

Gate particles are initially placed in a single row with a finer inter-particle spacing (dx/2, dz/2) to prevent particle penetration. Their velocities and positions are externally imposed to mimic the experimental movement of the gate according to ($V_x(t)$= 0.0 ms^{-1}; $V_z(t)$= 1.5 ms^{-1}).

4.3. NUMERICAL PARAMETERS

The parameter B in the equation of state (Batchelor, 1974) was chosen to guarantee that the speed of sound is a factor 10 larger than the velocities in the model. This can be achieved by taking $B = 100 g H_{ref} \rho_0 / \gamma$, where H_{ref} is the maximum water height in the tank (0.15 m in the numerical experiments). The viscosity term given by Monaghan (1992) was calculated using α= 0.08 and β= 0. In addition, fluid particles were moved using the so called XSPH (Monaghan, 1989) with ε= 0.5.

The numerical tank was 9 m long and 0.16 m deep.

4.4. TIME STEPPING

The Verlet algorithm (Verlet, 1967), was used in our numerical simulations. The basic idea of the algorithm is to write two third-order Taylor expansions for the positions, one forward and one backward in time:

$$\mathbf{r}(t+\Delta t) = \mathbf{r}(t) + \mathbf{v}(t)\Delta t + (1/2)\mathbf{a}(t)\Delta t^2 \qquad \mathbf{v}(t+\Delta t) = \mathbf{v}(t) + 2 \cdot \mathbf{a}(t)\Delta t^2 \tag{2}$$

Time-step control involves the Courant condition, the force terms and the viscous diffusion term (Monaghan, 1989). A variable time step δt was calculated according to (Monaghan and Kos, 1999):

$$\delta t = 0.3 \cdot \min(\delta t_f, \delta t_{cv}) \qquad \delta t_f = \min_a \left(\sqrt{\frac{h}{|\mathbf{f}_a|}} \right) \qquad \delta t_{cv} = \min_a \frac{h}{c_s + \max_b \left| \frac{h \mathbf{v}_{ab} \mathbf{r}_{ab}}{\mathbf{r}_{ab}^2} \right|} \tag{3}$$

Here δt_f is based on the force per unit mass **f**, and δt_{cv} combines the Courant and the viscous time-step controls. Typically, during the numerical runs, the time step decreases as the water velocity and the force per unit mass increase.

5. MODEL VALIDATION

5.1. WAVE PROFILES

Experimental wave profiles (Janosi *et al.* 2004) were digitized in order to be compared with SPH profiles. The dimensions of the digitized snapshots are 0.38 m ≤ X ≤ 1.04 m and 0.0 m ≤ Z ≤ 0.13 m. Distances were measured from the left-lower corner of the tank.

In Figure 2, *d*= 0.038 m was considered to compare numerical results and experiments. Experimental values are represented by dots and SPH values by a line. The model is observed to reproduce the experimental profile. In the first snapshot, the water initially placed behind the gate pushes the still water; second and third snapshots show the wave propagation and breaking.

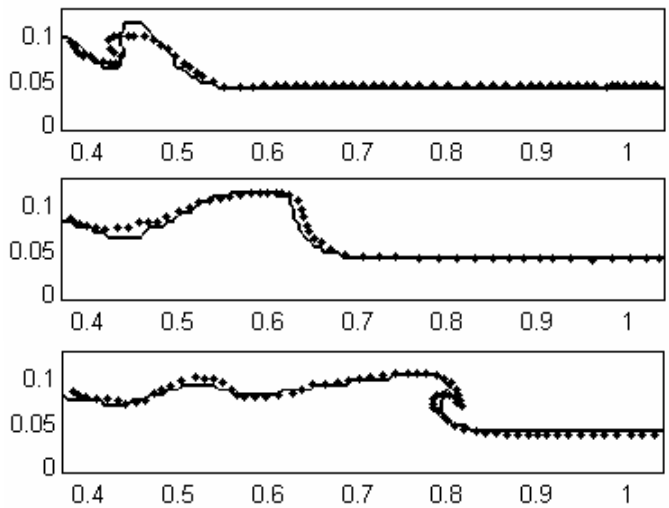

Figure 2: Comparison between experimental and numerical profiles of dam-break evolution over a wet bed (d=0.038m).

Apart from this visual comparison, the observed difference between numerical and experimental results can be quantified considering two statistical parameters:

$$A = \sqrt{\sum_{i=1}^{N} \left(Val_i^{num}\right)^2 \Big/ \sum_{i=1}^{N} \left(Val_i^{\exp}\right)^2} \qquad P = \sqrt{\sum_{i=1}^{N} \left(Val_i^{num} - Val_i^{\exp}\right)^2 \Big/ \sum_{i=1}^{N} \left(Val_i^{\exp}\right)^2}$$

A perfect agreement between both signals should result in $\boldsymbol{A} \rightarrow 1$ and $\boldsymbol{P} \rightarrow 0$. The good results obtained for *d*= 0.038 m (Figure 2: A = 1.012, P = 0.058) show the accuracy of the method.

5.2. WAVE VELOCITY

The experimental and numerical velocities were averaged along the first 3 meters of the tank (Figure 3). Numerically, the position of the leading edge was calculated every 0.06 s and

velocity was obtained by linear fitting. Both velocities and distances are depicted in a dimensionless form. Velocity is normalized considering $c = \sqrt{gd_0}$ and d/d_0 is the ratio between the depth of the fluid layer near bed and the initial dam height.

The normalized velocity is observed to decrease with d. The agreement between experimental measurements (light dots) and numerical results (dark squares) is excellent in most of the cases. Note that SPH velocity for dry bed is higher than observed in experiments, since experiments were not performed on a real dry bed, due to the impossibility of drying completely the tank.

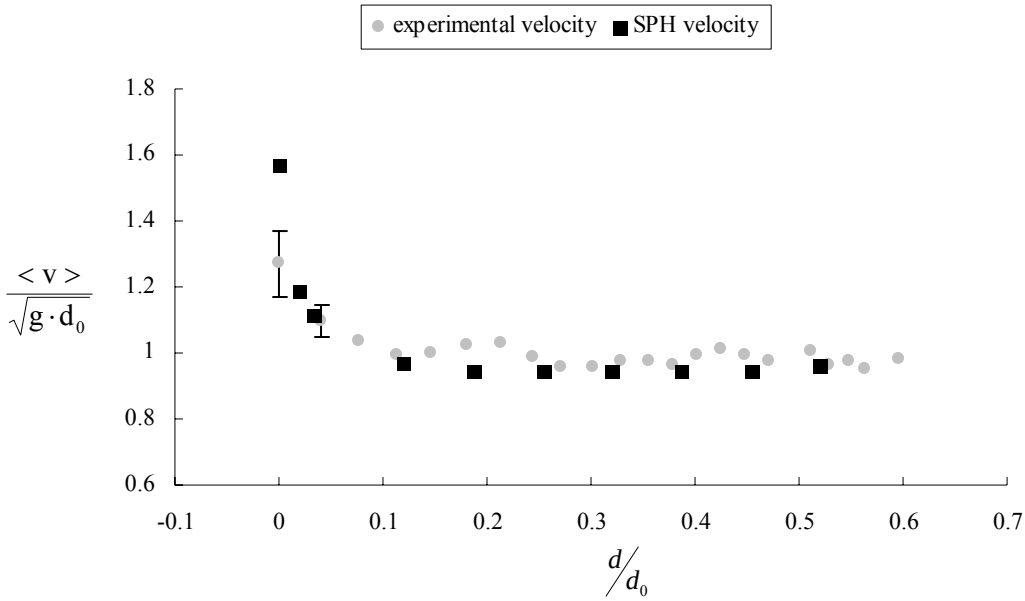

Figure 3: Comparison between experimental and numerical dam-break velocity.
The velocity was averaged during the first 3 m in both cases

6. DAM-BREAK ANALYSIS

Now that SPH has been shown to provide accurate results on dam break propagation, it can be used to analyze the dynamics of that propagation:

6.1. DAM BREAK EVOLUTION

The advance of a dam-break on a wet bed is far from being a stationary process, especially at the beginning of the movement, where the interaction between both fluids gives rise to different behaviors depending on the rate d/d_0 as previously shown. Thus, different propagation regimes can be observed depending on the zone, being the observed horizontal velocity considerably faster along the first 3 meters (dark squares in Figure 4) than along the first 6 meters (light circles in Figure 4).

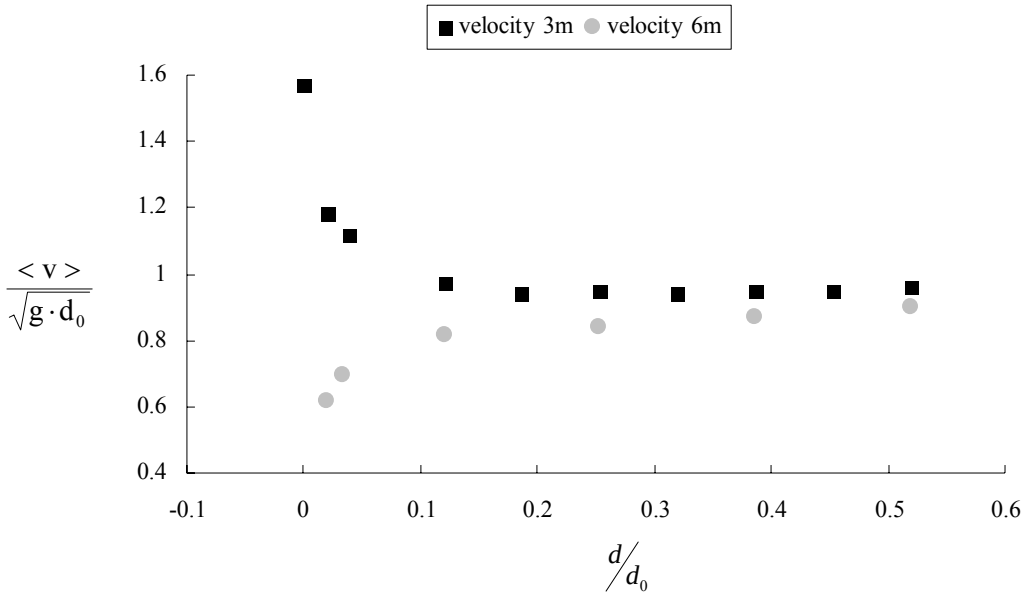

Figure 4: Average velocity along the first 3 meters and the first 6 meters for different fluid depths.

6.2. ENERGY DISSIPATION

The transition between both propagation regimes can be studied in terms of the dissipated energy. This energy can be defined as:

$$\Delta E(t) = \left(\sum_{i=1}^{N} E_i^{kinetic}(t=0) + \sum_{i=1}^{N} E_i^{potential}(t=0) \right) - \left(\sum_{i=1}^{N} E_i^{kinetic}(t) + \sum_{i=1}^{N} E_i^{potential}(t) \right)$$

where N is the number of fluid particles. Note that this definition (in terms of an increment) allows comparing different experiments, where the amount of fluid and, hence, the number of fluid particles is different.

Figure 5 shows the energy dissipated in different experiments over a wet bed (d=0.018 m; 0.038 m; 0.058 m; 0.078 m) and over a dry bed (d=0 m). Energy dissipation is observed to increase in time in all cases. In addition, when considering experiments over a wet bed, the energy dissipation measured at each particular instant is observed to be higher for small *d* values, decreasing monotonically with *d*. The behavior observed over a dry bed is completely different, energy dissipation measured at the beginning of the movement is lower than in the rest of the cases, since the interaction between both fluids constitutes the dominant dissipation mechanism. However, bottom friction becomes in time the main dissipation mechanism, in such a way that energy dissipation becomes higher over a dry bed than over wet beds.

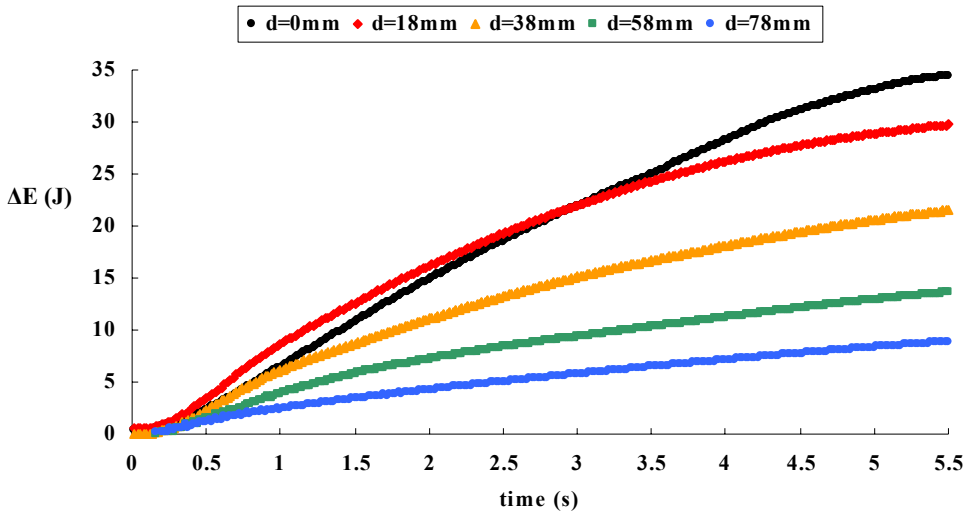

Figure 5: Energy dissipation for different *d* values.

7. VORTICITY

As SPH is a lagrangian method, the trajectories of each particle is known every instant and the vorticity of particle *a* is estimated by Monaghan, 1992:

$$\mathbf{w}_a = (\nabla \times \mathbf{v})_a = \sum_b m_b \frac{\mathbf{v}_a - \mathbf{v}_b}{\rho_a} \nabla W_{ab}$$

Next figures show the Y-component of vorticity (constant plane perpendicular to X and Z direction, see Fig. 1). Positive vorticity values (red colors) correspond to clock wise rotation and negative ones (dark blue colors) correspond to counter clock wise rotation. The dimensions of the snapshots are 0.0 m ≤ X ≤ 1.6 m and 0.0 m ≤ Z ≤ 0.16 m.

Firstly, vorticity was calculated in dam-break evolution for dry bed (Fig. 6.1). Highest negative values appear in the tip of the dam and positive values appear near bed due to bottom friction.

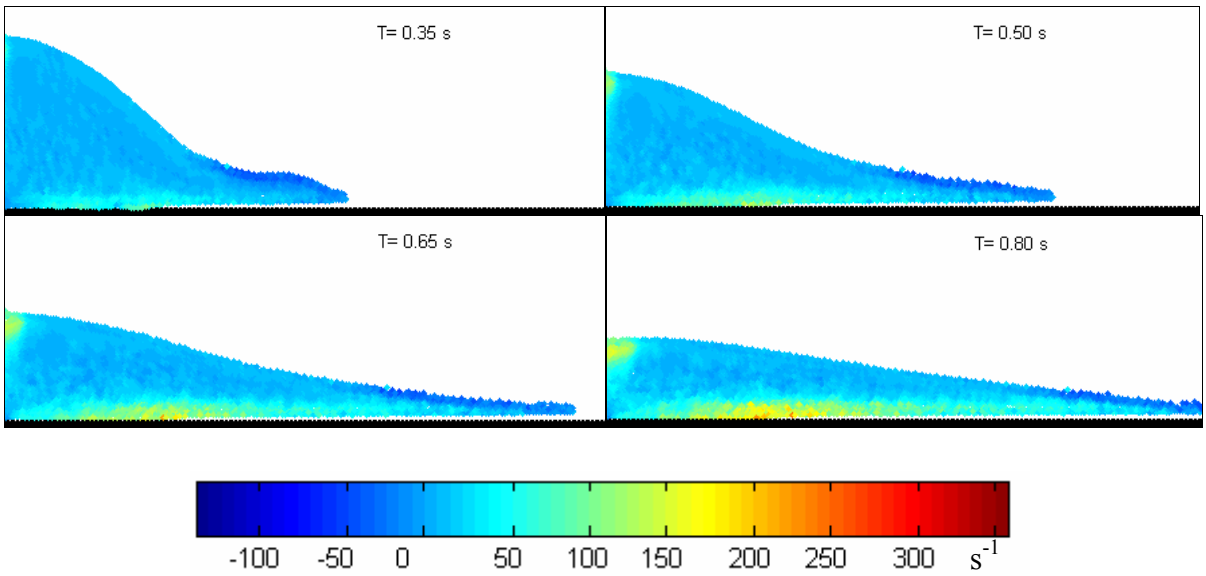

Figure 6.1: Vorticity plot for d=0.0 m.

Analyzing different instants for d=0.018 m (Fig. 6.2), the wave formation is observed in this case. The water initially placed behind the gate pushes the initially still water (first snapshot), generating the "mushroom" jet mentioned by Janosi *et al.* (2004). Negative vorticity appears on the left side of this "mushroom" (dark blue color) due to counter clock- wise water rotation. T=0.35s shows first breaking, that then generates the first positive eddy (red color in T=0.50s). T=0.65s shows the second breaking that is going to generate a second positive eddy (red colors in T=0.80s).

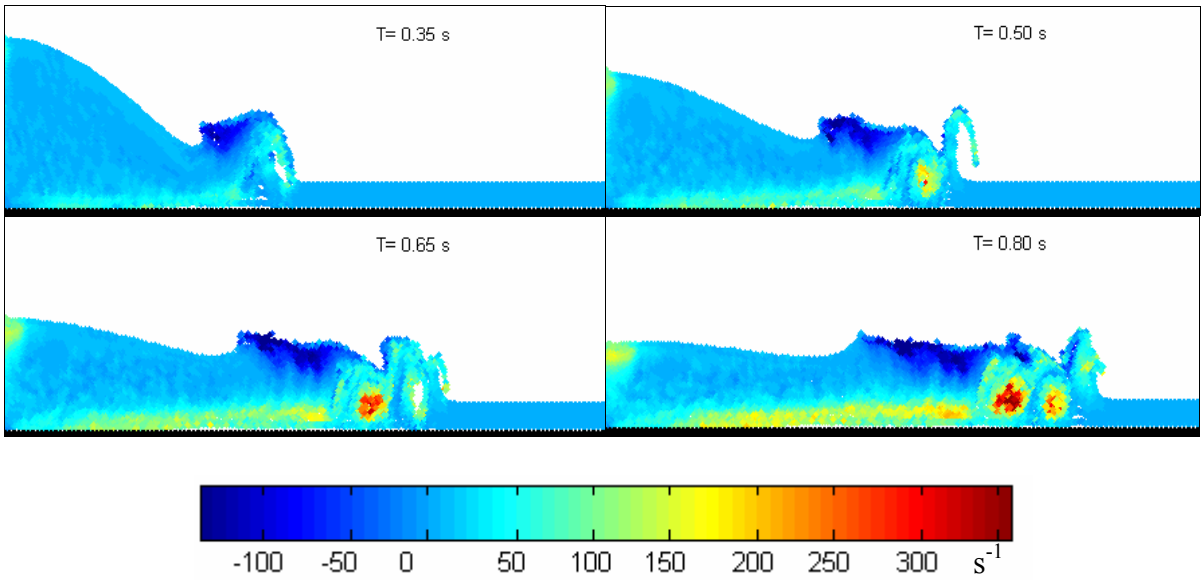

Figure 6.2: Vorticity plot for d=0.018 m.

Vorticity for d=0.058 m is also calculated (Fig. 6.3). Positive values appear mainly near bed due to close to bottom friction. There is not a wave breaking so there are not positive eddies. Water initially placed behind the gate pushes the still water initially placed beyond the gate without significant mixing. The interface of two water masses is clear and it coincides with the negative vorticity (dark blue colors).

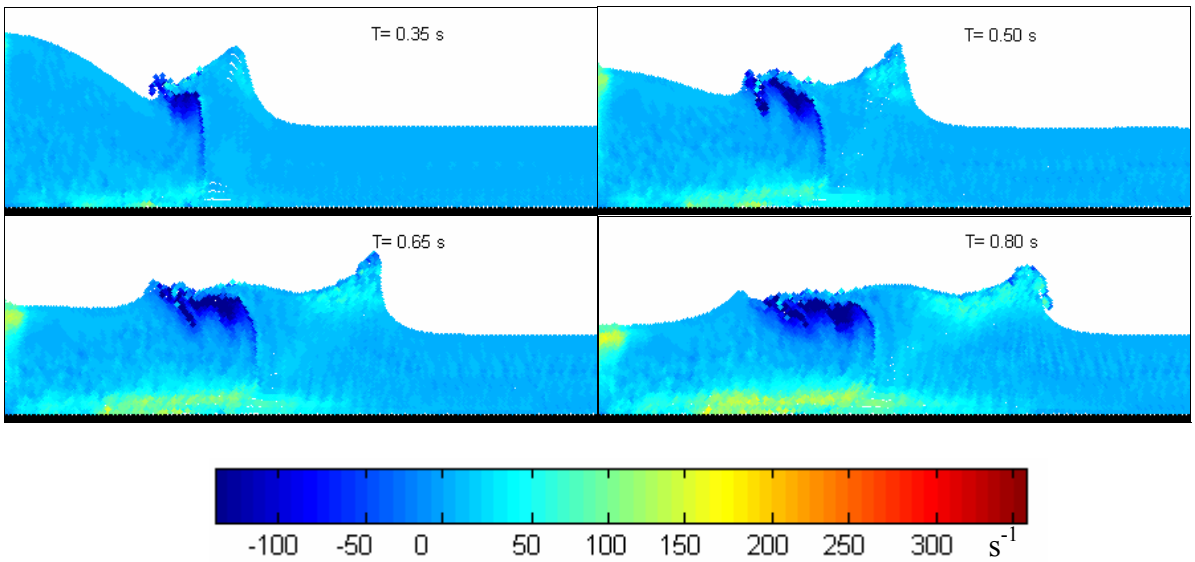

Figure 6.3: Vorticity plot for d=0.058 m.

The influence of XSPH on vorticity can also be taken in account, since the limit values vary depending on the value of ε. Although ε=0.5 is generally used in our simulations following Monaghan (1989), other values can also be considered. In particular ε=0 (no XSPH correction) was considered showing the same macroscopic vorticity pattern as the base case (ε=0.5). However, the limit values were observed to increase (in absolute value) in around 10% in the case without XSPH correction. All graphics in the text were calculated following the formulation given by Monaghan (1989) with ε=0.5, since this value provides the best fit in position and velocity to the experimental values with only a slight vorticity oversmoothing.

8. CONCLUSIONS

The 2D version of the SPH model has proven to be a suitable tool to reproduce a dam break evolution over dry and wet beds. Experimental profiles and horizontal velocities are properly reproduced by the model.

Two regimes are defined in dam evolution. Initial propagation (dam release) in horizontal direction is faster than observed for longer distances where velocity is mainly reduced by bottom friction. The difference between both regimes is higher for dry beds and shallow water layers.

Energy dissipation was observed to be responsible of both regimes. Energy dissipation for wet beds is higher at the beginning of the experiments, since breaking constitutes the main dissipation mechanism. However, bottom friction becomes in time the main dissipation mechanism, which is especially important on dry beds.

Vorticity is shown to depend on the fluid depth (d). Thus, when the dam-break propagates over a dry bed positive vorticity is mainly observed near bed due to bottom friction. Low negative values are only observed at the leading tip. Vorticity over a wet bed depends on water height: eddy formation with positive vorticity is observed for $d << d_0$ due to wave breaking. Negative vorticity is also observed in this case due to the so called "mushroom" jet. The breaking process is stopped when increasing d, in such a way that negative vorticity is only observed at the interface between both fluids.

REFERENCES

Batchelor, G. K. 1974. *Introduction to fluid dynamics*. Cambridge University Press. U.K.

Benz, W. 1990. Smoothed particle hydrodynamics: A review in *The numerical Modelling of Nonlinear Stellar Pulsations: Problems and Prspects*, J.R. Butchler ed., Kluwer Acad. Publ. 269-288.

Chanson, H., Aoki, S.and Maruyama, M. 2003. An experimental study of tsunami runup on dry and wet horizontal coastlines. *Science of Tsunami Hazards*, 20(5): 278- 293.

Dalrymple, R.A., Knio, O, Cox, D.T., Gómez-Gesteira, M., and Zou, S. 2002. Using a Lagrangian particle method for deck overtopping. *Proceedings of Waves 2001*, ASCE. 1082-1091.

Dressler, R.F. 1952. Hydraulic resistence effect upon the dam-break functions. *Journal of Research of the National Bureau of Standards*, 49(3): 217- 225.

Fontaine, E. 2000. On the use of smoothed particle hydrodynamics to model extreme waves and their interaction with structures. *Proceedings of Rogue Waves 2000*, Brest, France. www.ifremer.fr/metocean /conferences/wk.html.

Gingold, R. A. and Monaghan, J.J. 1977. Smoothed particle hydrodynamics: theory and application to non- spherical stars. *Mon. Not. R. Astr. Soc.*, 181: 375- 389.

Gómez-Gesteira, M. and Dalrymple, R. 2004. Using a 3D SPH Method for Wave Impact on a Tall Structure. *J. Wtrwy. Port, Coastal and Ocean Engrg.* 130(2): 63-69.

Gómez-Gesteira, M., Cerqueiro, D., Crespo, C., and Dalrymple, R. 2005. Green water overtopping analyzed with a SPH model, *Ocean Engineering.* 32: 223-238.

Henderson, F.M. 1966. Open channel flow. *Macmillan Company*, New York, USA.

Janosi, I. M., Jan, D., Szabo, K. G. and Tel, Tamas. 2004. Turbulent drag reduction in dam-break flows. *Experiments in Fluids,* 37: 219-229.

Klemp J.B., Rotunno R., Skamarock W.C. 1997. On the propagation of internal bores. *J Fluid Mech* 331:81–106

Liu, G.R. 2003. *Mesh Free methods: Moving beyond the finite element method*. CRC Press, pp. 692.

Lucy, L. 1977. A numerical approach to the testing of fusion process. *Journal Astronomical*, 82: 1013-1024.

Monaghan, J. J. 1982. Why particle methods work. *Siam J. Sci. Stat. Comput*., 3: 422-433.

Monaghan, J. J. and Latanzio, J.C. 1985. A refined method for astrophysical problems. *Astron. Astrophys*, 149: 135- 143.

Monaghan, J. J. 1989. On the Problem of Penetration in Particle Methods. *Journal Computational Physics*, 82: 1-15.

Monaghan, J. J. 1992. Smoothed particle hydrodynamics. *Annual Rev. Astron. Appl.*, 30: 543-574.

Monaghan, J. J., Cas, R. F., Kos, A., and Hallworth, M. 1999. Gravity currents descending a ramp in a stratified tank. *Journal Fluid Mechanics*, 379: 39-70.

Monaghan, J. J. 2000. SPH without Tensile Instability. *Journal Computational Physics,* 159: 290-311.

Monaghan, J. J. 2005. Smoothed particle hydrodynamics, *Reports on Progress in Physics*, 68: 1703-1759.

Montes, J.S. 1988. Hydraulics of open channel flow. *ASCE Press*, New- York.

Ritter, A. 1892. Die Fortpflanzung der Wasserwellen. *Zeitschrift des Vereines Deutscher Ingenieure* 36(24): 947- 954.

Verlet, L. 1967. Computer Experiments on Classical Fluids. I. Thermodynamical Properties of Lennard-Jones Molecules. *Phys. Rev*. 159: 98-103.

Whitham, G.B. 1955. The effects of hydraulic resistance in the dam- break problem. *Proc. Roy. Soc of London,* Ser. A, 227: 399-407.